

# Dynamic evolution characteristics of mining-induced fractures in overlying strata detected by radon

ZHANG Wei<sup>1,\*</sup> ZHANG Dongsheng<sup>1,2</sup> MA Liqiang<sup>1</sup> WANG Xufeng<sup>1</sup> FAN Gangwei<sup>1</sup>

<sup>1</sup>State Key Laboratory of Coal Resources and Safe Mining, School of Mines, China University of Mining & Technology, Xuzhou 221116, China

<sup>2</sup>College of Geology and Exploration Engineering, Xinjiang University, Urumchi 830046, China

**Abstract** For environment protection in mining areas in northwest China, we developed a CTSRM (comprehensive test system by radon measurement) to measure radon radioactivity and detect dynamic evolution characteristics of mining-induced fractures in overlying strata. It was used to simulate the relationship between the dynamic evolution characteristics and radon concentrations of 33201# coalface at Bulianta coal mine in Inner Mongolia, and feasibility of the method was validate.

**Key words** Radon detection, Comprehensive test system, Mining-induced fractures, Physical simulation

## 1 Introduction

As a key energy source in China, coal is of great importance for the nation's economic development. Many coal mines in northwest China, however, are located in the arid and semi-arid areas with shallow coal seams, in vulnerable surface ecological environment<sup>[1–3]</sup>. A large-scale mining with long wall coalfaces has been adopted in northwest China, which would cause mining-induced fractures in overlying strata<sup>[4,5]</sup>, resulting in environment problems of ground cracking, water resource loss, surface vegetation death, spontaneous combustion of coal seams, and desertification. Accurate monitoring of dynamic evolution of the mining-induced fractures in overlying strata is important for environment protection<sup>[6]</sup>.

Radon diffuses in the overlying strata and the migration distance depends on lithological characters. For example, vertical migration distance of radon in homogeneous sand is 360–420 m<sup>[7]</sup>. Rohnsch *et al.*<sup>[8]</sup> found abnormal radon concentration in surface soil of a deep shaft mining area. Jin Z X *et al.*<sup>[9]</sup> observed the increased radon concentration in a spontaneous coal combustion area at 400 m depth. These show radon

migration to surface from coal seam of 400–500 m depth, and radon detection can be used in shallow coal seam in northwest China.

The migrated radon can be accumulated in micropores and microfractures<sup>[10]</sup>. In measuring radioactivity of radon to detect dynamic evolution characteristics of mining-induced fractures in overlying strata, we developed a comprehensive test system by radon measurement (CTSRM) for reliable and effective radon monitoring.

## 2 Materials and Methods

### 2.1 The CTSRM

The CTSRM consists of mainly the adjustable 2D/3D physical simulation test-bed frame (PSTF), radon output device, circle pump, and KJD-2000R continuous emanometer (Fig.1).

The PSTF is made from channel steels. The visual mobile flashboard matching with the three symmetrical slots is installed at 0.5, 1.0 and 2.0 m in the width, so as to realize PSTF free transition from 2D to 3D model. Twenty-five radon cavities are laid at the bottom of PSTF, and dense micropores are set on the upper surface of each radon cavity. The radon

Supported by the National Natural Science Foundation of China (50904063 and 51004101), the Fundamental Research Funds for the Central Universities (2010ZDP02B02), and the State Key Laboratory of Coal Resources and Safe Mining (SKLCRSM08X02).

\* Corresponding author. E-mail address: zhangwei@cumt.edu.cn

Received date: 2011-06-08

cavities, radon output device and circulation pump are connected by  $\Phi 10$  mm plastic hoses. The Jack devices installed symmetrically at the lower surface of each radon cavity are used to control their lifting height. Some of the radon-monitoring positions are connected to KJD-2000R continuous emanometer by  $\Phi 5$  mm rubber hoses.

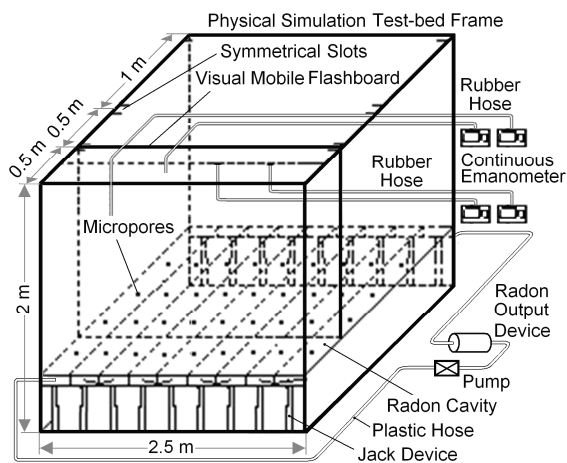


**Fig.1** Schematics of the CTSRM.

## 2.2 The physical simulation experiment

The CTSRM was used for physical simulation of the 32201<sup>#</sup> coalface conditions at Bulianta Coal Mine of Shendong Mining Area, Inner Mongolia, China, for correlating the dynamic evolution characteristics of mining-induced fractures in overlying strata with the radon concentration.

### 2.2.1 Geological conditions

The 32201<sup>#</sup> coalface is the first mining workface of 2<sup>-2#</sup> coal seam in Bulianta Coal Mine, of 240-m length and an average thickness of 5.5 m, at about 130-m depth. It is a typical shallow coal seam, of simple geological structures, with the surface being thick eolian sand.

### 2.2.2 Parameters of the physical model

In a ratio of 1:100, the physical model is sized at 2.5 m ( $l$ ) $\times$ 0.5 m ( $w$ ) $\times$ 1.21 m ( $h$ ). The model simulates the 250-m coalface, and the Jack devices lowered to 5.5 cm simulate the mining height of 5.5 m. There are eight simulation strata from 2<sup>-2#</sup> coal seam roof to surface, in a total thickness of 1.21 m. To eliminate boundary effect of the model, the coal pillar of 0.2 m width is retained at the two ends in strike direction. Then, the real mining length of physical model is 2.1

m. The 2<sup>-2#</sup> coal seam will be mined at one time per hour, with an advancing distance of 0.1 m. This stands for 10 m in actual coalface per day, therefore, the total mining time of the physical model is 21 h.

### 2.2.3 Choice of simulation materials

In the experiment, the unidirectional compressive strength of the overlying strata is considered as the main mechanical index. Therefore, a mixture of sand, calcium carbonate and gypsum were chosen as simulation materials. The thickness of the overlying strata and mating ratio of the materials are given in Table 1.

**Table 1** Thickness and materials ratio of the overlying strata.

Lithology	Thickness / m	Mating ratio*	Weight / kg
Aeolian sand	46	/	931.50
Sandstone	6	40:9:1	121.50
Mudstone	17	40:7:3	344.25
Packsand	20	40:3:7	405.00
Siltstone	10	60:7:3	202.50
Sandy mudstone	6	40:7:3	121.50
Packsand	10	30:3:7	202.50
Sandy mudstone	6	40:7:3	121.50
2 <sup>-2#</sup> coal	5.5	/	/
Sandy mudstone	5	/	/

\* Sand:calciumcarbonate:gypsum

### 2.2.4 Fabrication of similar model

Plastic films were pasted on inner surface of the PSTF to prevent radon from leaking. The PSTF was filled with the simulation materials, poured quickly into it and tamped by mechanical vibrator. Mica powder was used as natural layering boundaries in the neighboring strata. The model was completed in short time so as to avoid fast solidification of the materials.

### 2.2.5 Arrangement of monitoring points

Nine radon-monitoring positions were arranged in the model: six at the surface, while three at different depths to monitor radon content variation caused by evolution of mining-induced fractures. Monitoring positions in the middle section of the model were connected with the emanometers (Fig.2).

### 2.2.6 Mining process simulation

When the simulation materials achieved predetermined mechanical state and the radon concentration balanced, the mining process simulation

was carried out (Fig.3). Each radon cavity standing for 10-m coalface advancing was lifted down by 5.5 cm by adjusting the jack devices. The qualitative evolution characteristics of mining-induced fractures in overlying strata were observed by the visual mobile dashboard. Radon content at each monitoring position was recorded per 5 min.

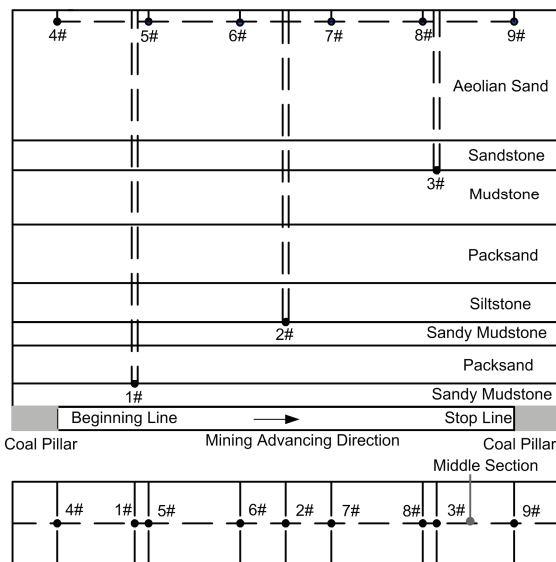


**Fig.2** Arrangement of monitoring positions.



**Fig.3** Mining process simulation.

### 3 Results and Discussion

Positions 1 and 5 were chosen for data processing. The results are shown in Fig.4, using the mining progress of the coalface as abscissa and the radon concentration at the monitoring points as ordinate. Being at the top boundary of the immediate roof, Position 1 was 6.0 m from the 2<sup>2#</sup> coal seam and 40-m beyond the beginning line. As shown in Fig.4(a), the initial radon concentration was 6672 Bq/m<sup>3</sup> before the coal seam

mining. It grew slowly until a coalface advancing of about 40-m, where it rose sharply up to reach peak of 11900 Bq/m<sup>3</sup> and the first age main roof break could be thus predicted, which was confirmed by qualitative observation of the visual mobile dashboard. Then, the radon concentration decreased slowly with the coalface advancing, and the mining-induced fractures in the caving zone closed up, with an average radon content of 7400 Bq/m<sup>3</sup> at the end.

Position 5 was 1.0-cm depth model, buried under the surface of aeolian sand and located at 42-m from the beginning line. As shown in Fig.4(b), due to radon migration caused by mining-induced fractures the radon content increased gradually from about 500 Bq/m<sup>3</sup> at the beginning. When coalface advanced to about 155 m, the overlying strata breaks, and radon content increased quickly to a maximum that was averaged at 2040 Bq/m<sup>3</sup> in the 180–220 m region, indicating that the mining-induced fractures in overlying strata expanded to the surface aeolian sand. The surface fractures closed up until the coalface advancing to the stop line. This was confirmed, too, by qualitative observation from the visual mobile dashboard.

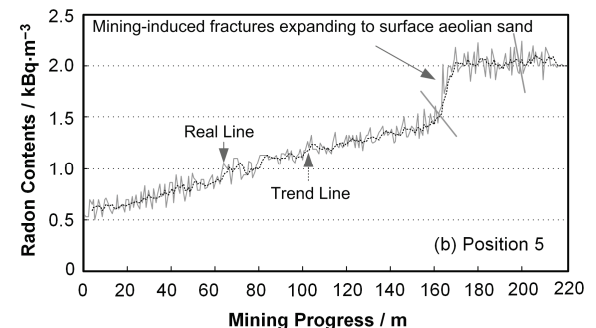
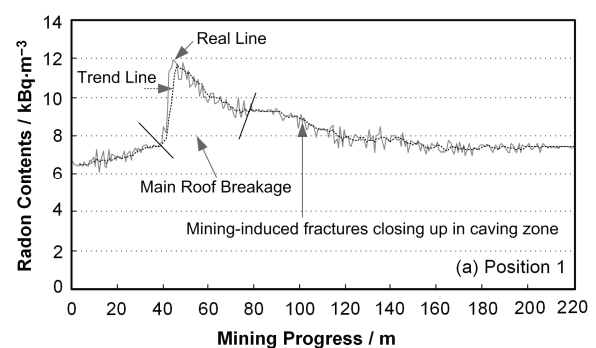


**Fig.4** Radon concentrations of (a) Position 1 and (b) Position 5.

#### 4 Conclusions

We developed a comprehensive test system by radon measurement (CTSRM) to detect dynamic evolution of mining-induced fractures in overlying strata. As a convenient physical model for fast 2D or 3D simulation, the system was applied in 2D physical simulation for 33201# coalface of Bulianta Coal Mine in Inner Mongolia. The relationship between the dynamic evolution of mining-induced fractures in overlying strata and radon concentrations during the 2<sup>-2#</sup> coal seam was studied, and feasibility of the method was validated.

#### References

- 1 Wang Y P, Shao M G, Zhang X C. *Acta Ecol Sini*, 2008, **28**: 3769–3778.
- 2 Cao S X. *Crit Revi Envi Sci & Tech*, 2011, **41**: 317–335.
- 3 Yang H K, Fan L M. *Coal Geol Expl*, 2003, **31**: 6–8.(in Chinese)
- 4 Zhang D S, Ma L Q, Wang X F, et al. *Proc Eart Plan Sci*, 2009, **1**: 60–67.
- 5 Ma L Q, Zhang D S, Jing S G, et al. *J China Univ Min Tech*, 2008, **18(3)**: 347–352.
- 6 Fan G W, Zhang D S, Ma L Q. *J China Univ Min Tech*, 2011, **40**: 196–201.(in Chinese)
- 7 Lennart M, Mats I, Krister K. *Geoe*, 1989, **26**: 135–144.
- 8 Rohnsch W, Przyborowski S, Ettenhuber E. *Radi Prot Dosi*, 1992, **45(S)**: 127–132.
- 9 Jin Z X, Bai X J, Wang A G. *J Nort China Inst Sci Tech*, 2006, **3**: 9–13.(in Chinese)
- 10 Ciotoli G, Etiope G, Guerra M, et al. *Quar J Eng Geol Hydr*, 2005, **38**: 305–320.